Crustal deformation of the eastern Tibetan plateau revealed by magnetotelluric imaging

Denghai Bai[1]*, Martyn J. Unsworth[2], Max A. Meju[3], Xiaobing Ma[1], Jiwen Teng[1], Xiangru Kong[1], Yi Sun[4], Jie Sun[5], Lifeng Wang[5], Chaosong Jiang[6], Ciping Zhao[6], Pengfei Xiao[1] and Mei Liu[1]

The ongoing collision of the Indian and Asian continents has created the Himalaya and Tibetan plateau through a range of deformation processes. These include crustal thickening, detachment of the lower lithosphere from the plate (delamination) and flow in a weakened lower crust[1–6]. Debate continues as to which of these processes are most significant[7]. In eastern Tibet, large-scale motion of the surface occurs, but the nature of deformation at depth remains unresolved. A large-scale crustal flow channel has been proposed as an explanation for regional uplift in eastern Tibet[6,8,9], but existing geophysical data[10,11] do not constrain the pattern of flow. Magnetotellurics uses naturally occurring electromagnetic waves to image the Earth's subsurface. Here we present magnetotelluric data that image two major zones or channels of high electrical conductivity at a depth of 20-40 km. The channels extend horizontally more than 800 km from the Tibetan plateau into southwest China. The electrical properties of the channels imply an elevated fluid content consistent with a weak crust[12,13] that permits flow on a geological timescale. These findings support the hypothesis that crustal flow can occur in orogenic belts and contribute to uplift of plateaux. Our results reveal the previously unknown complexities of these patterns of crustal flow.

Many previous studies of the India–Asia collision zone took place on the southern boundary of the Tibetan plateau in the Himalaya. However, the deformation of the eastern margin of the plateau is also important to developing a full understanding of this continent–continent collision (Fig. 1). Geologic[1] and geodetic studies[14] confirm that crustal blocks move clockwise around the eastern Himalayan syntaxis (EHS). Deformation at mid-crustal levels is not directly constrained by geodetic measurements and motion may be different from that observed at the surface. Seismic studies indicate that the crust and mantle might move coherently around the EHS (ref. 15). Geological studies in southeast Tibet indicate that the region of high elevation between the Sichuan basin and the EHS may have been uplifted with only small amounts of internal deformation[6,8]. It has been suggested that this uplift has been caused by an influx of lower crustal flow, as shown in Fig. 1. In this type of deformation, the flow is forced around regions of thick, stable lithosphere such as the Sichuan basin.

Geophysical imaging of the subsurface structure is needed to determine whether crustal flow is active in a region such as eastern Tibet. It is anticipated that such a flow channel would be characterized by a reduced seismic velocity and an elevated electrical conductivity (reduced resistivity), compared with stable continental crust. Seismic exploration in eastern Tibet has detected a widespread crustal low-velocity zone, with its upper surface at depths of 15–25 km, that was interpreted as a layer of aqueous fluids and/or partial melt[10,11]. This low-velocity layer was spatially variable and thinned to the southeast, but the large inter-station spacing did not permit detailed images of the inferred flow channel.

Magnetotelluric exploration can determine the electrical resistivity (or its reciprocal quantity, conductivity) of the crust and upper mantle. Conductivity is important in studies of crustal structure because it is sensitive to the presence of fluids. Magnetotelluric studies in southern Tibet gave images of a southward-directed crustal flow channel[12] and showed that the fluid content of the crust inferred from the magnetotelluric data was consistent with rheological conditions required for crustal flow[13]. The crustal flow pattern proposed for eastern Tibet[6,8] is geographically distinct from that inferred in southern Tibet and occurring over a larger horizontal scale. Magnetotelluric data on the INDEPTH-600 line in northern Tibet[16] and on profile P3 in Sichuan[17] (Fig. 1) detected a layer with elevated mid-crustal conductivity that may represent fluid-rich regions associated with crustal flow. However, the distance between these two magnetotelluric surveys was too large to reliably correlate features from one profile to another. This Letter describes the results of a new magnetotelluric survey in eastern Tibet that has detected two major zones of high-crustal-conductivity crust that seem to be parts of a regionally extensive layer, and which are inferred to be zones with elevated fluid content where deformation occurs most rapidly.

Broadband magnetotelluric data were recorded between 2004 and 2007 at 325 locations in the eastern Himalaya syntaxis (EHS3D) survey with a total profile length of 2,110 km (Fig. 1). Details of the magnetotelluric data analysis are presented in the Supplementary Information. Geoelectric strike directions were computed using tensor decomposition[18] and were found to be generally parallel to major surface geological features. The relatively two-dimensional (2D) nature of the magnetotelluric data permitted the application of 2D inversion[19] to generate electrical resistivity/conductivity models for each profile (Fig. 2a). In each model the upper crust has a high electrical resistivity (low conductivity), which is typical of dry crustal rocks. The most conspicuous feature in the models is a layer of elevated conductivity in the mid-crust, beginning at an average depth of 25 km. The conductivity of the layer varies horizontally, and there are two regions with very high conductivity. Beneath this conductive layer, the lithosphere seems to have a lower conductivity, although magnetotelluric data cannot reliably locate the base of such a conductive layer. Near-surface zones of low resistivity are coincident with major strike-slip faults[20] and
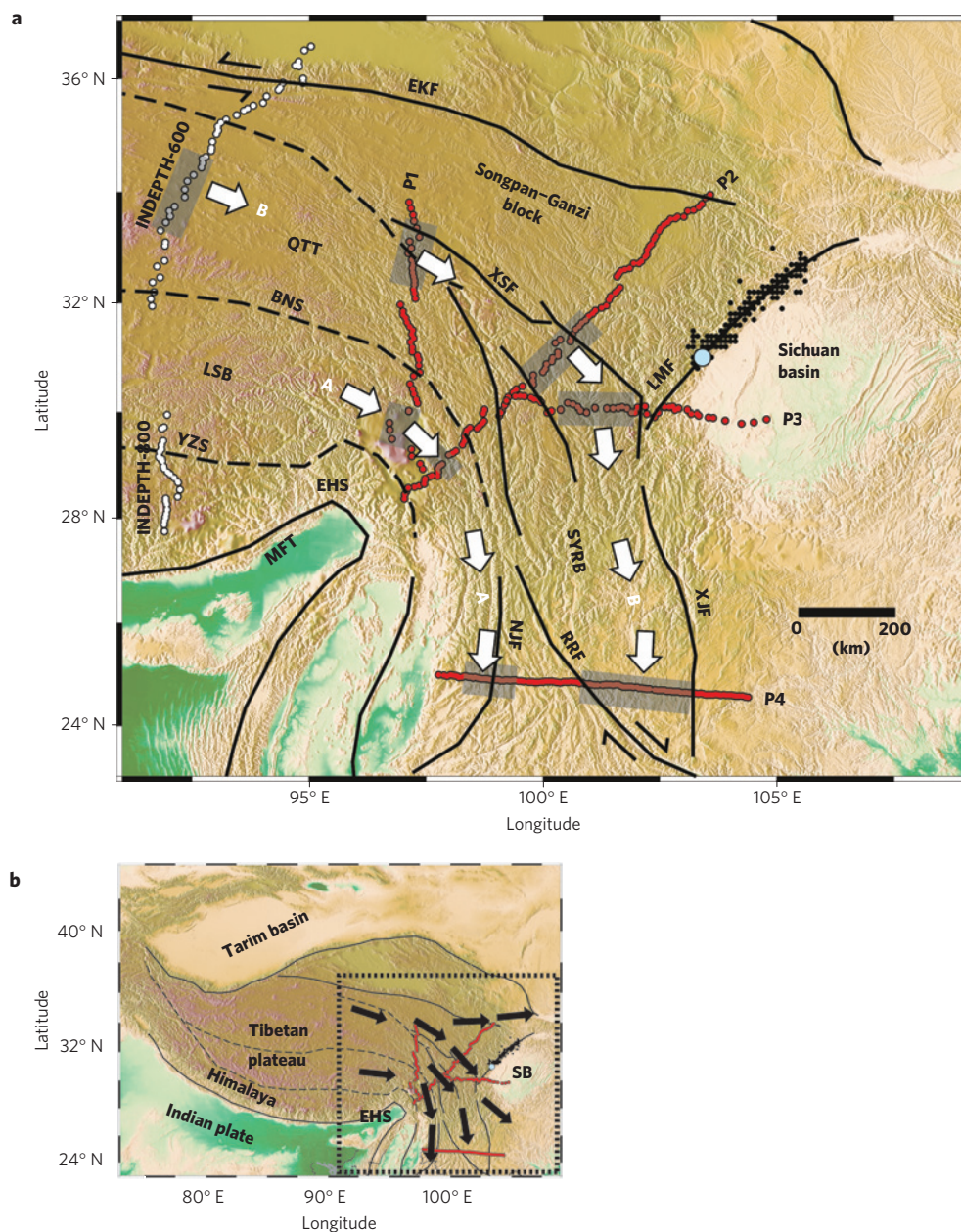
Figure 1 | Map showing surface relief of the eastern Tibetan plateau and the adjacent area. a, The red dots denote magnetotelluric stations and the shaded rectangles are regions of the magnetotelluric profiles with high crustal conductance (>10,000 S). P1–P4 denote the magnetotelluric profiles EHS3D-3, EHS3D-2, CZMT-WE and EHS3D-1, respectively. The light blue dot shows the epicentre of the 2008 Wenchuan $M = 7.9$ earthquake and the black dots show major aftershocks. BNS = Bangong–Nujiang suture; EHS = eastern Himalayan syntaxis; EKF = east Kunlun fault; LMF = Longmenshan fault; LSB = Lhasa block; MFT = main frontal thrust; NJF = Nujiang fault; QTT = QiangTang terrane; RRF = Red River fault; SB = Sichuan basin; SYRB = Sichuan–Yunnan rhombic block; XJF = Xiaojiang fault; XSF = Xianshuihe fault; YZS = Yarlung–Zangbo suture; A and B denote the two zones with the highest conductance. The white arrows connect the regions of highest conductance and inferred location of flow channels. **b**, Regional setting. The black arrows define the pattern of lower crustal flow proposed to explain the topographic slope[8].

regions with geothermal phenomena[21]. Zones of elevated mid-crustal conductivity have previously been reported in Tibet and other active orogens, and have been attributed to the presence of either aqueous fluids or partial melts[22–24]. The presence of fluids is significant because it weakens the crust and may define regions where crustal flow could occur[13]. The new magnetotelluric data set in eastern Tibet has a large spatial extent, and the distribution of the high-conductivity layer provides information to understand the spatial distribution of deformation in eastern Tibet[8,9].

Magnetotelluric data are primarily sensitive to the depth-integrated conductivity of a layer (conductance), and not to the individual values of conductivity and thickness. Therefore, the data analysis was focused on the spatial variations in the conductance of the conductive mid-crustal layer. The conductance of this layer was computed using a constrained 2D inversion in which the lithosphere below a specified depth was forced to have a low conductivity. A range of depths was chosen and the final layer conductance was found to be insensitive to the choice of value in the range 50–100 km. Note that Fig. 2a shows the unconstrained inversions. The conductance of the layer in the final model was computed, with shallow features excluded from the integration. The conductance values shown in Fig. 2b are 1–2 orders of magnitude
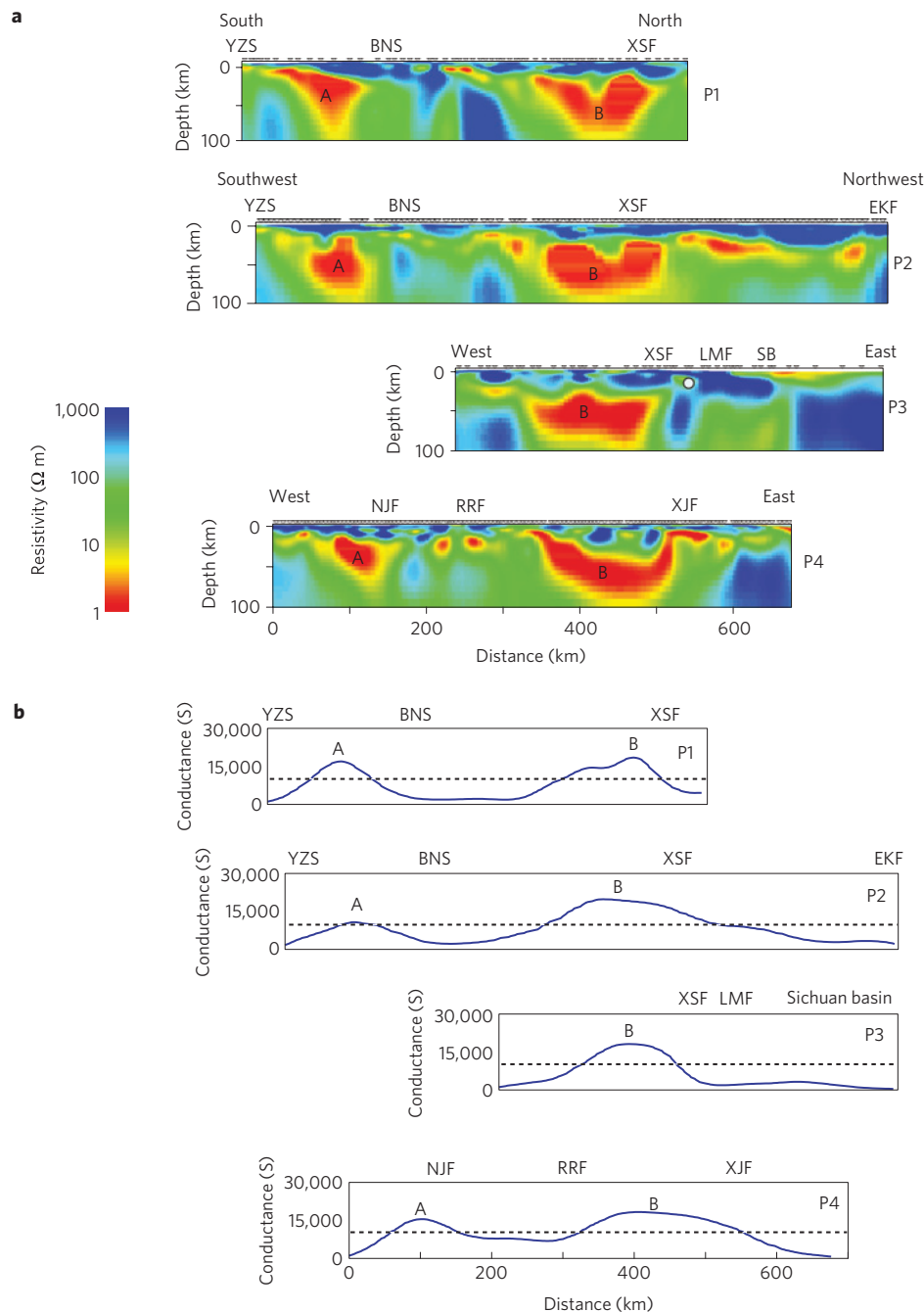
Figure 2 | Electrical resistivity cross-sections for eastern Tibet. a, Resistivity models for the magnetotelluric profiles shown in Fig. 1. **b**, The solid line shows the conductance of the model constrained to be resistive below 60 km depth. Similar conductance values were obtained when the inversion was unconstrained. For abbreviations see Fig. 1. The dashed line shows a conductance of 10,000 S.

higher than those found in regions of stable continental crust (200–500 S) and locally exceed 20,000 S. Figure 2 shows two zones of high conductance that can be correlated between the EHS3D profiles. The western conductive zone (A) is located close to the EHS and the eastern conductive zone (B) follows the surface trace of the Xianshuihe and Xiaojiang faults.

To use these models to constrain the pattern of deformation in eastern Tibet, it is first necessary to compute the quantity of fluids required to produce the observed crustal conductance. Elevated crustal conductivities can be due to thermal effects, aqueous fluids, partial melt, mineralization or graphite[22]. The large spatial extent of A and B probably excludes metallic mineralization as an explanation. The dominant effect of increasing temperature

occurs when melting causes a significant increase in conductivity. The preferred explanation for the high conductivity in a region of active tectonics is some combination of aqueous fluids and/or partial melt[5,22]. The conductance can be used to estimate the volume of fluid/melt that is present in the crust. Laboratory experiments show that pure melts have an electrical conductivity in the range 3–10 S m^{-1} (resistivity 0.1–0.3 Ω m), whereas aqueous fluids have slightly higher conductivity values[25]. The geometric distribution of the fluid within the pore space of the rock controls the bulk conductivity, and laboratory studies indicate that a high degree of interconnection may occur in partial melts and aqueous fluids[26]. The values of fluid content (porosity) and layer thickness required to produce a given conductance can be computed (Fig. 3). Note
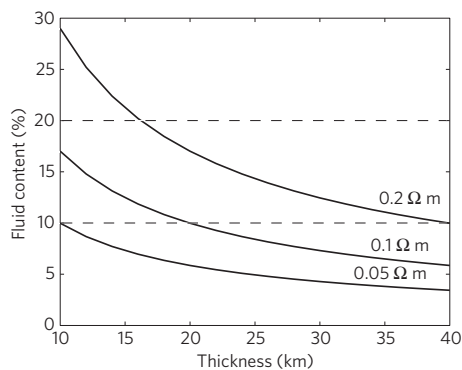
Figure 3 | Variation of thickness and fluid content (porosity) for a crustal layer with a conductance of 10,000 S. The three curves used values of resistivity for a fluid phase of 0.05, 0.1 and 0.2 Ω m. The fluid is assumed to be relatively well interconnected and the bulk resistivity is estimated with Archie's Law.

Figure 4 | Fluid content (porosity) of a 20-km-thick mid-crustal layer required to account for the conductance of profiles P1 and P4. The three curves use values of resistivity for the pure fluid phase of 0.05, 0.1 and 0.2 Ω m respectively. The fluid is assumed to be well interconnected and the bulk resistivity is estimated with Archie's Law.

that, as the layer thickness increases, the fluid fraction required to give a particular conductance decreases.

The conductance values can be used to give quantitative estimates of fluid content along each EHS3D profile. This requires an extra constraint to overcome the inherent trade-off between thickness and fluid content. If it is assumed that the conductor has a thickness of 20 km, on the basis of the thickness of seismic low-velocity zones[10,11], then the required fluid content can be computed (Fig. 4). In zones A and B a fluid content of 5–20% is required to account for the observed conductivity. A fluid content greater than 5% is sufficient to produce a factor of 10 strength reduction compared with the surrounding material with the same composition[13]. Geodynamic modelling indicates that this strength contrast is sufficient for crustal flow to occur[4]. Analysis of the mechanical and electrical properties of a fluid-rich layer has shown that flow velocities increase with conductance, and conductance values greater than 7,000–10,000 S correspond to average flow rates of 1 cm yr^{-1} (ref. 27). The fluids could be derived from prograde metamorphism in a thickened crust or from underplating. The spatial extent of A and B supports the idea that they are channels of flow, because their boundaries avoid stable regions, such as the Sichuan basin, predicted to be barriers to crustal flow[8,9]. For example, the northern extent of the low-resistivity zone B coincides with the East Kunlun fault (P2 in Fig. 2), and its eastern limit on P3 coincides with the Xianshuihe fault and the western edge of the Sichuan basin. Although not well sampled, it seems that the conductor terminates at the southwest end of line P2, near the Yarlung–Zangbo suture.

The fact that the high conductivity is localized in two channels (A and B) indicates a more complex pattern of deformation than the crustal flow previously suggested[8]. The properties of A and B, described in the previous section, are consistent with flow occurring in these channels. In contrast, the relatively high resistivity of the mid-crust between A and B does not require an elevated fluid content, and the arguments presented above suggest a weak mid-crustal layer is absent. Seismic measurements show that the crust and upper mantle are mechanically coupled and deform coherently[15]. Together these arguments suggest that zones A and B could also act as shear zones that permit the relative motion of lithospheric blocks. Laboratory studies have shown that shearing of mid and lower crustal rocks will form and maintain a network of aligned, interconnected fluid-filled cracks[28]. This change in fluid distribution will also enhance the conductivity of these regions. Further evidence for A and B being shear zones comes from the observation that on profiles P2 and P4, the conductors are located where the horizontal surface velocity changes most rapidly.
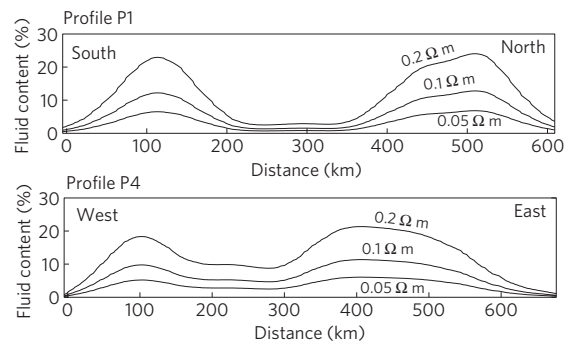
The conductivity models in Fig. 2 reveal a more complex pattern of deformation than that previously suggested. The high fluid content required for localized crustal flow occurs at the edges of the deformation zone, indicating that deformation may include both crustal flow and shearing in zones A and B. Recent numerical modelling has indicated that this style of crustal flow is difficult to maintain[29]. It is possible that the shearing may be required to maintain regions with sufficient interconnected fluid to lower the crustal strength and permit rapid deformation. The $M = 8.0$ Wenchuan earthquake occurred in the Longmenshan region on 12 May 2008 (ref. 30). The EHS3D profiles presented in this letter did not pass directly through the rupture zone of the Wenchuan earthquake. However, the models reveal that magnetotelluric studies can potentially contribute to understanding the mechanism that caused this earthquake.

References

1. Tapponnier, P. *et al*. Oblique stepwise rise and growth of the Tibetan plateau. *Science* **294,** 1671–1677 (2001).
2. Yin, A. & Harrison, T. M. Geologic evolution of the Himalayan–Tibetan orogen. *Annu. Rev. Earth Planet. Sci.* **28,** 211–280 (2000).
3. DeCelles, P. G., Robinson, D. M. & Zandt, G. Implications of shortening in the Himalayan fold-thrust belt for uplift of the Tibetan plateau. *Tectonics* **21,** 1062 (2002).
4. Beaumont, C., Jamieson, R. A., Nguyen, M. H. & Lee, B. Himalayan tectonics explained by extrusion of a low-viscosity crustal channel coupled to focused surface denudation. *Nature* **414,** 738–742 (2001).
5. Klemperer, S. L. in *Channel Flow, Ductile Extrusion and Exhumation in Continental Collision Zones* Vol. 268 (eds Law, R. D., Searle, M. P. & Godin, L.) 39–70 (Geological Society, Special Publications, 2006).
6. Royden, L. H. *et al*. Surface deformation and lower crustal flow in eastern Tibet. *Science* **276,** 788–790 (1997).
7. Replumaz, A. & Tapponnier, P. Reconstruction of the deformed collision zone between India and Asia by backward motion of lithospheric blocks. *J. Geophys. Res.* **108,** 2285 (2003).
8. Clark, M. K. & Royden, L. H. Topographic ooze: Building the eastern margin of Tibet by lower crustal flow. *Geology* **28,** 703–706 (2000).
9. Copley, A. & McKenzie, D. Models of crustal flow in the India–Asia collision zone. *Geophys. J. Int.* **169,** 683–698 (2007).
10. Yao, H., Beghein, C. & van der Hilst, R. Surface wave array tomography in SE Tibet from ambient seismic noise and two-station analysis—II. Crustal and upper-mantle structure. *Geophys. J. Int.* **173,** 205–219 (2008).
11. Xu, L., Rondenay, S. & van der Hilst, R. Structure of the crust beneath the southeastern Tibetan plateau from teleseismic receiver functions. *Phys. Earth Planet. Inter.* **165,** 176–193 (2007).
12. Unsworth, M. J. *et al*. Crustal rheology of the Himalaya and southern Tibet inferred from magnetotelluric data. *Nature* **438,** 78–81 (2005).
13. Rosenberg, C. L. & Handy, M. R. Experimental deformation of partially melted granite revisited: Implications for the continental crust. *J. Metamorphic Geol.* **555,** 1–9 (2005).

14. Zhang, P. *et al.* Continuous deformation of the Tibetan plateau from global positioning system data. *Geology* **32,** 809–812 (2004).
15. Sol, S. *et al.* Geodynamics of the southeastern Tibetan plateau from seismic anisotropy and geodesy. *Geology* **35,** 563–566 (2007).
16. Unsworth, M. J. *et al.* Crustal and upper mantle structure of northern Tibet imaged with magnetotelluric data. *J. Geophys. Res.* **109,** B02403 (2004).
17. Sun, J., Jin, G., Bai, D. & Wang, L. Sounding of electrical structure of the crust and upper mantle along the eastern border of Qinghai–Tibet plateau and its tectonic significance. *Sci. China* **46,** 243–253 (2003).
18. McNeice, G. M. & Jones, A. G. Multisite, multifrequency tensor decomposition of magnetotelluric data. *Geophysics* **66,** 158–173 (2001).
19. Rodi, W. & Mackie, R. L. Nonlinear conjugate gradients algorithm for 2D magnetotelluric inversion. *Geophysics* **66,** 174–187 (2001).
20. Leloup, P. H. *et al.* New constraints on the structure, thermochronology and time of the Ailao Shan–Red River shear zone, Southeast Asia. *J. Geophys. Res.* **106,** 6683–6732 (2001).
21. Hochstein, M. P. & Regenauer-Lieb, K. Heat generation associated with collision of two plates: The Himalayan geothermal belt. *J. Volcanol. Geotherm. Res.* **83,** 75–92 (1998).
22. Li, S. *et al.* Partial melt or aqueous fluid in the mid-crust of southern Tibet? Constraints from INDEPTH magnetotelluric data. *Geophys. J. Int.* **153,** 289–304 (2003).
23. Brasse, H. *et al.* The Bolivian Altiplano conductivity anomaly. *J. Geophys. Res.* **107,** 2096 (2002).
24. Türkoğlu, E., Unsworth, M. J., Çağlar, İ., Tuncer, V. & Avşar, Ü. Lithospheric structure of the Arabia–Eurasia collision zone in eastern Anatolia from magnetotelluric exploration: Evidence for widespread weakening by fluids. *Geology* **36,** 619–622 (2008).
25. Nesbitt, B. Electrical resistivities of crustal fluids. *J. Geophys. Res.* **98,** 4301–4310 (1993).
26. ten Grotenhuis, S. M., Drury, M. R., Spiers, C. J. & Peach, C. J. Melt distribution in olivine rocks based on electrical conductivity measurements. *J. Geophys. Res.* **110,** B12201 (2005).
27. Rippe, D. & Unsworth, M. J. Quantifying crustal flow in Tibet with magnetotelluric data. *Phys. Earth Planet. Inter.* **179,** 107–121 (2010).
28. Tullis, J., Yund, R. & Farver, J. Deformation enhanced fluid distribution in feldspar aggregates and implications for ductile shear zones. *Geology* **24,** 63–66 (1996).
29. Teyssier, C., Whitney, D. L & Rey, P. F. The rheologic implications of partial melting in Continental plateaux. *Eos. Trans. AGU (Fall Meeting Suppl.)* **90,** abstr. T32C-07 (2009).
30. Burchfiel, B. C. *et al.* A geological and geophysical context for the Wenchuan earthquake of 12 May 2008, Sichuan, People's Republic of China. *GSA Today* **18,** 4–11 (2008).

Author contributions

D.B. designed the project, collected and interpreted data and wrote the paper. M.J.U. processed and interpreted data and wrote the paper. M.A.M. designed the project, interpreted data and wrote the paper. X.M. and Y.S. designed the project and processed data. J.T., X.K., J.S. and C.J. designed the project and interpreted data. L.W. and C.Z. designed the project and collected data. P.X. and M.L. collected the data.